

Quantization Robustness of Monotone Operator Equilibrium Networks

James Li¹, Philip H.W. Leong¹ and Thomas Chaffey¹

Abstract—Monotone operator equilibrium networks are implicit-layer models whose output is the unique equilibrium of a monotone operator, guaranteeing existence, uniqueness, and convergence. When deployed on low-precision hardware, weights are quantized, potentially destroying these guarantees. We analyze weight quantization as a spectral perturbation of the underlying monotone inclusion. Convergence of the quantized solver is guaranteed whenever the spectral-norm weight perturbation is smaller than the monotonicity margin; the displacement between quantized and full-precision equilibria is bounded in terms of the perturbation size and margin; and a condition number characterizing the ratio of the operator norm to the margin links quantization precision to forward error. MNIST experiments confirm a phase transition at the predicted threshold: three- and four-bit post-training quantization diverge, while five-bit and above converge. The backward-pass guarantee enables quantization-aware training, which recovers provable convergence at four bits.

I. INTRODUCTION

Neural networks now underpin modern machine learning, from vision and language to decision and control. Contemporary models often contain millions or billions of parameters, increasing compute and memory demands and constraining deployment in embedded and latency-sensitive settings. This motivates **quantization**, which reduces memory footprint and accelerates training and inference by representing weights and activations at low-bit precision [1]. Lower precision enables efficient integer arithmetic but introduces quantization (rounding) errors that grow as bit-width decreases. Analytic bounds relating quantization error to a network’s robustness and stability would let bit-width be selected based on deployment requirements rather than by trial and error.

This motivates the question of whether quantization error can be bounded at the model level. At present, there is no generally applicable bound on quantization error; instead, only architecture-specific analyses exist [2], [3]. Progress therefore requires restricting attention to architectures with tractable convergence guarantees — a requirement familiar in control, where quantized feedback has been modeled as a sector-bounded perturbation and stability is analyzed via small-gain conditions [4]. **Monotone operator equilibrium networks** (MonDEQs) [5] are a class of deep equilibrium models (DEQs) [6] that enforce monotonicity of the underlying operator, guaranteeing existence, uniqueness, and linear convergence of the equilibrium via operator splitting. The built-in monotonicity constraints of MonDEQs make

them suitable as controllers with formal stability and robustness guarantees [7], [8], and they can be realized in energy-efficient analog hardware [9]. A MonDEQ layer’s well-posedness is captured by a single spectral margin: the smallest eigenvalue m of a symmetric matrix constructed from the layer’s weights (defined formally in Section II). Having $m > 0$ ensures that the implicit equation defining the layer has a unique equilibrium and that the numerical solver converges to it. Because quantization perturbs this matrix and hence its eigenvalues, the monotonicity margin m provides a natural handle for analyzing quantization error. Thus far, MonDEQs have only been treated in full-precision arithmetic; to the best of our knowledge, what happens to the convergence guarantee under quantization has not been analyzed.

A. Contributions

The contributions of this paper are as follows.

- 1) We formalize quantization error in a MonDEQ as a bounded spectral-norm perturbation of the weight matrix and derive the induced perturbation of the monotonicity margin and Lipschitz constant (Theorem 2, Section IV-A).
- 2) We give explicit conditions under which the quantized MonDEQ retains existence, uniqueness, and linear convergence of its equilibrium (Corollary 1, Section IV-A).
- 3) We bound the fixed-point displacement between quantized and full-precision equilibria and derive the associated condition number (Theorems 3–4, Section IV-B).
- 4) We show that the backward solve inherits the same convergence guarantees as the forward solve under quantization (Theorem 5, Section IV-C).

We demonstrate these contributions empirically across bit-widths from 3 to 32 bits on MNIST (Section V). To support reproducible research, the code is available at <https://github.com/JLi-Projects/mondeq-quant>.

B. Related Work

Quantization theory. Standard quantization modeling treats the quantized weight matrix as a bounded perturbation of its full-precision counterpart [1], [10]. Post-training quantization (PTQ) applies a fixed quantizer after training, while quantization-aware training (QAT) incorporates the quantizer into the training loop via a straight-through estimator [11]. *Inexact operator splitting.* Operator splitting methods such as forward–backward and Peaceman–Rachford admit inexact variants in which bounded per-step errors are tolerated while preserving convergence [12], [13]. In Section IV, we apply

¹All authors are with the School of Electrical and Computer Engineering, The University of Sydney, NSW, Australia. Emails: {jali4795@uni.sydney.edu.au, {philip.leong, thomas.chaffey}@sydney.edu.au.

these results to quantization-induced errors in the MonDEQ solver and derive new bounds on equilibrium displacement and the associated condition number.

Numerical error analysis. Beuzeville et al. [14] show that feedforward networks are backward stable under floating-point rounding. Jonkman et al. [15] model quantized communication in distributed optimization as an inexact Krasnosel’skiĭ–Mann iteration.

MonDEQ sensitivity. Pabbaraju et al. [16] derive input-output and weight-output Lipschitz bounds for MonDEQs, but their perturbation bound assumes the perturbed margin is known and does not address quantization-specific structure, convergence conditions, or condition number.

II. PRELIMINARIES

We collect notation and standard definitions from monotone operator theory that are used throughout the paper.

We work in \mathbb{R}^n with the Euclidean norm $\|\cdot\|_2$ and denote the spectral norm of a matrix by $\|\cdot\|_2$. The symmetric and skew-symmetric components of a matrix A are $\text{sym}(A) := \frac{1}{2}(A + A^\top)$ and $\text{skw}(A) := \frac{1}{2}(A - A^\top)$.

Monotone operators. Given an operator $F : \mathbb{R}^n \rightarrow \mathbb{R}^n$, its graph, denoted $\text{gra}(F)$, is defined as $\{(x, y) \mid x \in \mathbb{R}^n, y = F(x)\}$. An operator $F : \mathbb{R}^n \rightarrow \mathbb{R}^n$ is said to be *monotone* if $\langle F(x) - F(y), x - y \rangle \geq 0$ for all $x, y \in \mathbb{R}^n$, and *maximal* if its graph is not properly contained in the graph of any other monotone operator. Given $m, L > 0$, an operator $F : \mathbb{R}^n \rightarrow \mathbb{R}^n$ is said to be *m -strongly monotone* if $\langle F(x) - F(y), x - y \rangle \geq m\|x - y\|_2^2$ for all $x, y \in \mathbb{R}^n$, and *L -Lipschitz* if $\|F(x) - F(y)\|_2 \leq L\|x - y\|_2$ for all $x, y \in \mathbb{R}^n$. For the affine operator $F(z) = (I - W)z - (Ux + b)$, the strong monotonicity margin (also referred to simply as the margin) is $m = \lambda_{\min}(\text{sym}(I - W))$ and the Lipschitz constant is $L = \|I - W\|_2$ [17], [18].

Resolvents. For a maximal monotone operator G , the resolvent $J_{\alpha G} := (I + \alpha G)^{-1}$ is single-valued, firmly nonexpansive, and hence 1-Lipschitz. The reflected resolvent is $R_{\alpha G} := 2J_{\alpha G} - I$ [18].

The *forward-backward* iteration $z^{k+1} = J_{\alpha G}((I - \alpha F)z^k)$ converges linearly for any $\alpha \in (0, 2m/L^2)$ with contraction modulus $r_{\text{FB}} = \sqrt{1 - 2\alpha m + \alpha^2 L^2}$ [17], [18]. The *Peaceman-Rachford* iteration $z^{k+1} = (2J_{\alpha G} - I)(2J_{\alpha F} - I)z^k$ converges linearly for any $\alpha > 0$ with contraction modulus $\rho_{\text{PR}} = \sqrt{1 - \frac{4\alpha m}{(1 + \alpha L)^2}}$ [17], [18].

III. MONOTONE OPERATOR EQUILIBRIUM NETWORKS

Monotone operator equilibrium networks (MonDEQs) [5] compute their output as the fixed point of a splitting map derived from a monotone inclusion. We summarize the key definitions.

Definition 1. Fix an input $x \in \mathbb{R}^d$. Let $W \in \mathbb{R}^{n \times n}$, $U \in \mathbb{R}^{n \times d}$ and $b \in \mathbb{R}^n$ be parameters collected in a vector $\vartheta \in \mathbb{R}^r$. Let $\sigma : \mathbb{R} \rightarrow \mathbb{R}$ be the componentwise activation on \mathbb{R}^n . Define the affine map

$$F(z) := (I - W)z - (Ux + b), \quad z \in \mathbb{R}^n.$$

Let $G : \mathbb{R}^n \rightrightarrows \mathbb{R}^n$ be a maximal monotone operator and let $J_{\alpha G} := (I + \alpha G)^{-1}$ denote its resolvent for any $\alpha > 0$. Considering the nonlinear fixed point iteration

$$z^{k+1} = J_{\alpha G}(I - \alpha F)z^k := \Phi(z^k; \vartheta),$$

suppose it has a fixed point z^* . We call the mapping from the input x to fixed point z^* a **monotone operator equilibrium network (MonDEQ)**.

The following equivalence is established in [5].

Theorem 1. Define a MonDEQ as in Definition 1. Then $z^* \in \text{Fix}(\Phi) \iff 0 \in F(z^*) + G(z^*)$.

Theorem 1 reduces computation of the MonDEQ output to solving the monotone inclusion $0 \in F(z^*) + G(z^*)$. This reformulation is useful because the splitting algorithms of monotone operator theory apply directly and converge linearly when F is strongly monotone.

The following parameterization enforces $\text{sym}(I - W) \succeq mI$, so that F is m -strongly monotone.

Proposition 1. $\text{sym}(I - W) \succeq mI$ if and only if there exist $A, B \in \mathbb{R}^{n \times n}$ such that $W = (1 - m)I - A^\top A + B - B^\top$.

Proof. Direct computation [5]. \square

The margin m is determined by the parameterization of W . Because $m = \lambda_{\min}(\text{sym}(I - W))$ is an explicit function of W , perturbing the weight matrix perturbs m in a way that can be bounded analytically. Since $m > 0$ is both necessary and sufficient for well-posedness, bounding how quantization perturbs m directly determines whether the quantized network remains well-posed.

IV. QUANTIZATION IN A MONDEQ

Here, quantization replaces floating-point weights with fixed-point (low-bit) approximations, reducing memory and enabling efficient integer arithmetic at the cost of increased rounding error. We analyze the resulting error as a perturbation of the weight matrix $W \rightarrow \widetilde{W} = W + \Delta W$ [10], bounding its effect on well-posedness, the equilibrium point, and the backward pass used for training.

We use symmetric uniform (mid-tread) quantization: for b -bit representation with weights in $[-1, 1]$, the quantizer $Q_\Delta(w) = \Delta \cdot \text{round}(w/\Delta)$ has step size $\Delta = 2^{1-b}$ and worst-case elementwise error $\Delta/2$. Uniform quantization is standard for weight compression because the evenly spaced levels map directly to fixed-point integer formats, enabling hardware-accelerated matrix arithmetic; non-uniform schemes such as logarithmic quantizers [4] sacrifice this property. Since each entry of ΔW is bounded by $\Delta/2$, we have $\|\Delta W\|_2 \leq (\Delta/2)\sqrt{n^2}$. This motivates modeling weight quantization as a bounded perturbation [10].

Definition 2. Given a MonDEQ as in Definition 1, its quantized counterpart replaces W with $\widetilde{W} = W + \Delta W$, $\|\Delta W\|_2 \leq \varepsilon_W$.

For the symmetric uniform quantizer with step size $\Delta = 2^{1-b}$ at b bits, $\varepsilon_W = n\Delta/2$.

Weight quantization introduces a deterministic perturbation to the weight matrix. This raises the question of how large the perturbation can be before the equilibrium ceases to exist. In practice, each iterate also incurs computational errors such as finite-precision arithmetic or activation rounding, so the computed iterates obey $z^{k+1} = \tilde{\Phi}(z^k) + \delta_k$ with bounded per-step errors δ_k . Together, the weight perturbation ΔW and the iterate errors δ_k model the two sources of error in a quantized MonDEQ.

A. Margin Perturbation and Well-Posedness

The following theorem shows that weight perturbation reduces the monotonicity margin by at most $\|\Delta W\|_2$. This theorem is a special case of [19, Theorem 4].

Theorem 2. *Define a MonDEQ in accordance with Definition 1 with weights W satisfying Proposition 1. Let \tilde{W} be the quantized weights with perturbation $\|\Delta W\|_2 \leq \varepsilon_W$. Then the strong monotonicity margin \tilde{m} of \tilde{W} is bounded below by*

$$\tilde{m} \geq m - \|\Delta W\|_2,$$

and the Lipschitz constant \tilde{L} of \tilde{W} satisfies $|L - \|\Delta W\|_2| \leq \tilde{L} \leq L + \|\Delta W\|_2$.

Proof. Since $\tilde{W} = W + \Delta W$, we have $\text{sym}(I - \tilde{W}) = \text{sym}(I - W) - \text{sym}(\Delta W)$. By the Rayleigh-quotient characterization of extreme eigenvalues [20],

$$\begin{aligned} \tilde{m} &= \min_{\|x\|_2=1} x^\top [\text{sym}(I - W) - \text{sym}(\Delta W)] x \\ &\geq \min_{\|x\|_2=1} x^\top \text{sym}(I - W) x - \max_{\|x\|_2=1} x^\top \text{sym}(\Delta W) x \\ &\geq m - \|\text{sym}(\Delta W)\|_2 \geq m - \|\Delta W\|_2, \end{aligned}$$

where the last step uses $\|\text{sym}(\Delta W)\|_2 \leq \|\Delta W\|_2$. For the Lipschitz constant, the triangle and reverse triangle inequalities give

$$|L - \|\Delta W\|_2| \leq \tilde{L} = \|I - \tilde{W}\|_2 \leq L + \|\Delta W\|_2. \quad \square$$

It follows from the bound $\tilde{m} \geq m - \|\Delta W\|_2$ that if $\|\Delta W\|_2 < m$, then $\tilde{m} > 0$: when the weight perturbation is smaller than the monotonicity margin, the quantized operator remains strongly monotone and well-posedness is preserved. The Lipschitz bound cuts both ways: the upper bound means quantization can slow convergence, while the lower bound means the quantized operator may be better-conditioned if the perturbation reduces $\|I - W\|_2$. In the worst case, the condition number $\tilde{\kappa} = \tilde{L}/\tilde{m}$ degrades from both sides (m shrinks and L grows), so the solver requires more iterations and the equilibrium becomes more sensitive to further perturbation. In practice, the margin bound is the binding constraint. Since $\text{sym}(I - W) = mI + A^\top A$, the margin m (the minimum eigenvalue) is exactly attained wherever $A^\top A$ has a zero eigenvalue, making it directly exposed to perturbation. In contrast, the Lipschitz constant $L = \|I - W\|_2$ is robust to elementwise rounding errors. We state the contraction result for forward-backward splitting; an analogous result holds for Peaceman-Rachford splitting with $\rho_{\text{PR}}(\alpha; \tilde{m}, \tilde{L})$.

Corollary 1. *If $\varepsilon_W < m$, the quantized forward-backward map $\tilde{\Phi}_{\text{FB}} := J_{\alpha G} \circ (I - \alpha \tilde{F})$ is a contraction with modulus $r_{\text{FB}}(\alpha; \tilde{m}, \tilde{L})$.*

Proof. Replace (m, L) by (\tilde{m}, \tilde{L}) from Theorem 2 in the forward-backward convergence rate. \square

In words, weight quantization slows convergence but does not break it: the solver still reaches a unique equilibrium, and the next subsection bounds how far that equilibrium moves.

B. Equilibrium Displacement

The next result bounds how far the quantized equilibrium \tilde{z}^* moves from the full-precision equilibrium z^* .

Theorem 3. *Assume $F(z) = (I - W)z - (Ux + b)$ is m -strongly monotone and $G : \mathbb{R}^n \rightrightarrows \mathbb{R}^n$ is monotone. With \tilde{W} given as in Definition 2, suppose $\|\Delta W\|_2 < m$ (in particular $\tilde{m} > 0$). Let*

$$\tilde{F}(z) := (I - \tilde{W})z - (Ux + b) = F(z) - \Delta Wz.$$

Let z^* and \tilde{z}^* denote the (unique) solutions of the full-precision and quantized inclusions

$$0 \in F(z^*) + G(z^*), \quad 0 \in \tilde{F}(\tilde{z}^*) + G(\tilde{z}^*).$$

Then

$$\|\tilde{z}^* - z^*\|_2 \leq \frac{\|\Delta W\|_2}{m} \|\tilde{z}^*\|_2. \quad (1)$$

In particular, if $\Delta W = 0$ then $\tilde{z}^* = z^*$.

Proof. Pick $g^* \in G(z^*)$ and $\tilde{g}^* \in G(\tilde{z}^*)$ with $F(z^*) + g^* = 0$ and $\tilde{F}(\tilde{z}^*) + \tilde{g}^* = 0$. Subtracting and using $\tilde{F}(z) = F(z) - \Delta Wz$, then taking the inner product with $\delta z := \tilde{z}^* - z^*$ gives

$$\langle F(\tilde{z}^*) - F(z^*), \delta z \rangle - \langle \Delta W \tilde{z}^*, \delta z \rangle + \langle \tilde{g}^* - g^*, \delta z \rangle = 0.$$

By m -strong monotonicity of F , the first term is $\geq m\|\delta z\|_2^2$; by monotonicity of G the third is ≥ 0 . Hence

$$m\|\delta z\|_2^2 \leq \langle \Delta W \tilde{z}^*, \delta z \rangle \leq \|\Delta W\|_2 \|\tilde{z}^*\|_2 \|\delta z\|_2$$

by Cauchy-Schwarz. Dividing by $\|\delta z\|_2$ (the case $\delta z = 0$ is trivial) yields (1). \square

The bound (1) depends on $\|\tilde{z}^*\|_2$ rather than $\|z^*\|_2$ because the perturbation acts through the shifted fixed point. An explicit bound in terms of $\|z^*\|_2$ alone is given in Corollary 3.

The preceding results concern weight quantization, which shifts the equilibrium itself. In practice, a second error source arises: *iterate quantization*, where finite-precision arithmetic or activation rounding introduces per-step residuals during the solver iteration. The next result extends the convergence guarantee to this combined setting.

Corollary 2. *Let $\tilde{\Phi}$ be a quantized map as in Corollary 1, with contraction modulus $r \in (0, 1)$ and fixed point \tilde{z}^* . Then*

$$\limsup_{k \rightarrow \infty} \|z^k - \tilde{z}^*\|_2 \leq \frac{\limsup_{k \rightarrow \infty} \|\delta_k\|_2}{1 - r}.$$

If $\sum_{k=0}^{\infty} \|\delta_k\|_2 < \infty$, then $z^k \rightarrow \tilde{z}^*$ exactly.

Proof. Follows from standard inexact contraction results [18]. \square

In practice, bounded per-step errors (e.g. from finite-precision arithmetic) do not destroy convergence: the solver reaches a neighborhood of \tilde{z}^* whose radius is controlled by the error magnitude and contraction rate. The summability condition $\sum \|\delta_k\|_2 < \infty$ holds, for example, when an adaptive quantizer increases precision at each iteration so that $\|\delta_k\|_2$ decays geometrically [15].

The total error decomposes as $\|z^k - z^*\|_2 \leq \|z^k - \tilde{z}^*\|_2 + \|\tilde{z}^* - z^*\|_2$: the first term is governed by iterate errors (Corollary 2), the second by weight displacement (Theorem 3). With summable iterate errors, the first term vanishes, and the total error is determined by the displacement bound alone.

The bound (1) measures displacement in absolute terms. We now derive a relative bound and extract the condition number, which separates the problem's inherent sensitivity from the perturbation size.

Corollary 3. *Under the hypotheses of Theorem 3, if $\|\Delta W\|_2 < m$ then*

$$\frac{\|z^* - \tilde{z}^*\|_2}{\|z^*\|_2} \leq \frac{\|\Delta W\|_2}{m - \|\Delta W\|_2}. \quad (2)$$

Proof. From Theorem 3, $\|\tilde{z}^* - z^*\|_2 \leq \frac{\|\Delta W\|_2}{m} \|\tilde{z}^*\|_2$. Substituting $\|\tilde{z}^*\|_2 \leq \|z^*\|_2 + \|\tilde{z}^* - z^*\|_2$ gives $\|\tilde{z}^* - z^*\|_2 \leq \frac{\|\Delta W\|_2}{m} (\|z^*\|_2 + \|\tilde{z}^* - z^*\|_2)$. Rearranging, $(1 - \|\Delta W\|_2/m) \|\tilde{z}^* - z^*\|_2 \leq \frac{\|\Delta W\|_2}{m} \|z^*\|_2$, which yields (2) since $\|\Delta W\|_2 < m$. \square

Corollary 3 gives a global bound: the relative displacement is at most $\|\Delta W\|_2 / (m - \|\Delta W\|_2)$, which depends only on the perturbation size and margin. For example, at 8 bits ($\|\Delta W\|_2 = 0.035$, $m = 0.227$), the bound gives 18%; the empirical relative error is much smaller (Section V). As $\|\Delta W\|_2 \rightarrow 0$, the bound linearizes to $\|\Delta W\|_2/m$, recovering the condition number scaling of Theorem 4.

The sensitivity of the equilibrium to small weight perturbations is captured by the condition number [10], [21].

Theorem 4. *For an unquantized MonDEQ with margin $m > 0$, the absolute condition number*

$$\kappa_{\text{abs}} := \limsup_{\|\Delta W\|_2 \rightarrow 0} \frac{\|z^*(\tilde{W}) - z^*(W)\|_2}{\|\Delta W\|_2}$$

satisfies $\kappa_{\text{abs}} \leq \|z^*\|_2 / m$.

Proof. From Theorem 3, $\|z^* - \tilde{z}^*\|_2 / \|\Delta W\|_2 \leq \|\tilde{z}^*\|_2 / m$. By Corollary 3, $\|\tilde{z}^*\|_2 \leq \|z^*\|_2 / (1 - \|\Delta W\|_2/m)$, so $\|z^* - \tilde{z}^*\|_2 / \|\Delta W\|_2 \leq \|z^*\|_2 / (m - \|\Delta W\|_2)$. Taking $\|\Delta W\|_2 \rightarrow 0$ gives $\kappa_{\text{abs}} \leq \|z^*\|_2 / m$. \square

In words, the equilibrium's sensitivity to weight perturbation is governed by the ratio of its magnitude to the monotonicity margin. The corresponding relative condition number, which measures sensitivity to relative perturbations, is $\kappa_{\text{rel}} = \kappa_{\text{abs}} \cdot \|W\|_2 / \|z^*\|_2 \leq \|W\|_2 / m$, so that

$\|z^* - \tilde{z}^*\|_2 / \|z^*\|_2 \leq \kappa_{\text{rel}} \eta_W$ to first order, where $\eta_W := \|\Delta W\|_2 / \|W\|_2$ is the relative weight perturbation. For the trained MNIST model in Section V ($m = 0.227$, $\|W\|_2 = 1.72$), this gives $\kappa_{\text{rel}} \approx 7.6$: a 1% relative weight perturbation causes at most roughly 7.6% relative displacement.

To ensure stability under quantization, it suffices to verify that the actual perturbation satisfies $\|\Delta W\|_2 < m$. This is the condition of Theorem 2: it guarantees that the quantized operator retains strong monotonicity (and hence a unique equilibrium with guaranteed convergence). Since $\|\Delta W\|_2 \leq \varepsilon_W$, a sufficient pre-deployment check is $\varepsilon_W < m$, or equivalently $\eta_W < m / \|W\|_2$ in relative terms. Moreover, a single check ($\tilde{m} > 0$) guarantees convergence of both forward and backward passes (Theorem 5).

For feedforward networks, the computed output is the exact output of a network with perturbed weights [14], but the error accumulates through L layers as $O(Lu)$. For MonDEQs, contractivity bounds the error regardless of iteration count: the quantized equilibrium \tilde{z}^* is exact for the perturbed operator $I - \tilde{W}$, and the displacement is controlled by the condition number.

The results so far establish convergence and displacement bounds for the forward pass — the computation of the equilibrium \tilde{z}^* . For training, however, we also need the backward pass (implicit differentiation through the equilibrium) to converge. The following subsection shows that the backward inclusion has the same linear part $I - W$ as the forward problem, so it inherits the same margin, Lipschitz constant, and convergence guarantees.

C. Backward Pass Under Quantization

Training a MonDEQ requires computing gradients of the loss with respect to the parameters $\vartheta = (W, U, b)$, which involves implicit differentiation through the equilibrium condition $0 \in F(z^*; \vartheta) + G(z^*)$. Differentiating with respect to a scalar parameter component ϑ yields a backward inclusion whose linear part is $I - W$, the same operator that governs the forward problem [5]. More precisely, the backward sensitivity $p := \frac{dz^*}{d\vartheta}$ solves $0 \in (I - W)p - r + G_b(p)$, where $r := \frac{dW}{d\vartheta} z^* + \frac{dU}{d\vartheta} x + \frac{db}{d\vartheta}$ and $G_b \in \partial_C G(z^*)$ is a Clarke generalized Jacobian with $\text{sym}(G_b) \succeq 0$ [22]. Since the margin m and Lipschitz constant L are determined entirely by $I - W$, the backward pass inherits the same convergence guarantees as the forward pass. The following theorem shows that this structure is preserved under weight quantization.

Theorem 5. *Let $\tilde{W} = W + \Delta W$ with $\|\Delta W\|_2 < m$, and let \tilde{z}^* solve $0 \in \tilde{F}(\tilde{z}^*; \vartheta) + G(\tilde{z}^*)$. Define $\tilde{p} := \frac{d\tilde{z}^*}{d\vartheta}$, $\tilde{r} := \frac{d\tilde{W}}{d\vartheta} \tilde{z}^* + \frac{dU}{d\vartheta} x + \frac{db}{d\vartheta}$, and let $\tilde{G}_b \in \partial_C G(\tilde{z}^*)$ with $\text{sym}(\tilde{G}_b) \succeq 0$. Then \tilde{p} solves*

$$0 \in (I - \tilde{W})\tilde{p} - \tilde{r} + \tilde{G}_b(\tilde{p}), \quad (3)$$

and the splitting method converges to \tilde{p} with the perturbed parameters (\tilde{m}, \tilde{L}) from Theorem 2. In particular, if the forward pass converges ($\tilde{m} > 0$), then the backward pass also converges with the same contraction modulus; a single margin check suffices for both passes.

Proof. Differentiating $\tilde{F}(\tilde{z}^*; \vartheta) + \tilde{g}^* = 0$ with respect to ϑ yields (3). The backward operator $(I - \tilde{W})p - \tilde{r}$ has the same linear part as \tilde{F} , so it inherits the same (\tilde{m}, \tilde{L}) from Theorem 2. Since \tilde{G}_b is monotone by assumption, the same splitting method converges. \square

Theorem 5 validates quantization-aware training (QAT): whenever the forward pass converges under quantized weights, gradients can be computed at the same precision and with the same iteration budget. No additional solver resources are required for the backward pass.

The gradient error under quantization has two sources: the displaced equilibrium ($z^* \rightarrow \tilde{z}^*$) and the perturbed weight matrix ($W \rightarrow \tilde{W}$). By Theorem 5, the backward sensitivity \tilde{p} solves a monotone inclusion with the same linear operator $(I - \tilde{W})$, so the backward equilibrium exists and can be computed by the same splitting method. Since both sources introduce perturbations of size $O(\|\Delta W\|_2)$ (the weight perturbation directly, and the equilibrium displacement via Theorem 3), the chain rule gives $\left\| \frac{\partial \ell}{\partial W} - \frac{\partial \ell}{\partial \tilde{W}} \right\|_2 = O(\|\Delta W\|_2)$.

V. NUMERICAL EXPERIMENTS

We validate the theoretical predictions of Section IV on a single-layer MonDEQ with $n = 100$ hidden units, trained on MNIST using Adam ($\text{lr} = 10^{-3}$, 15 epochs, step decay $\gamma = 0.1$ at epoch 10). Unlike [5], which fixes m as a hyperparameter, we treat m as learnable via a softplus reparameterization ensuring $m > 0$. The trained model achieves 98.22% test accuracy with margin $m = 0.227$, Lipschitz constant $L = 1.845$, and condition number $\kappa = L/m = 8.13$. Post-training quantization (PTQ) applies symmetric uniform quantization with step size $\Delta = 2^{1-b}$ and per-tensor scaling to the weight matrix W , without calibration or bias correction [1], [11]. Quantization-aware training (QAT) retrains from random initialization with the same architecture and hyperparameters, using a straight-through estimator to pass gradients through the quantizer [11]. In both cases, the deployed model uses $\tilde{W} = Q(W)$, so the perturbation model of Definition 2 applies. The forward-backward solver terminates when the relative residual falls below 10^{-5} or after 2000 iterations.

Margin stability certificate. Figure 1 tests the convergence condition $\|\Delta W\|_2 < m$ from Theorem 2 across bit-widths from 3 to 32 bits. The transition from non-convergence to convergence aligns with the predicted threshold $\|\Delta W\|_2/m = 1$: 3-bit ($\|\Delta W\|_2/m = 5.36$) and 4-bit (2.66) fail to converge, while 5-bit and above converge. The 5-bit case ($\|\Delta W\|_2/m = 1.25$) illustrates that the condition is sufficient but not necessary: the actual margin $\tilde{m} = 0.045 > 0$, so the quantized operator remains strongly monotone and the solver converges despite the sufficient condition being violated. The iteration count reflects the degraded margin: 5-bit requires ~ 1730 iterations (near the 2000 cap), while 8-bit converges in ~ 450 . At 8 bits, weight storage is reduced $4\times$ compared with single-precision floating-point, with negligible accuracy change (98.24% vs. 98.22%).

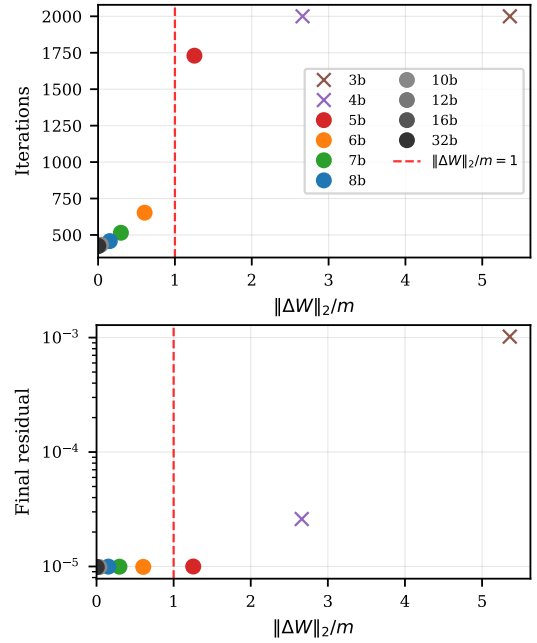


Fig. 1. Margin stability certificate. Iterations to convergence (top) and final residual (bottom) vs. normalized perturbation $\|\Delta W\|_2/m$; each point is one bit-width (3–32 bits). The dashed line marks the sufficient condition $\|\Delta W\|_2/m = 1$. Circles: converged (relative residual $< 10^{-5}$); crosses: did not converge within 2000 iterations.

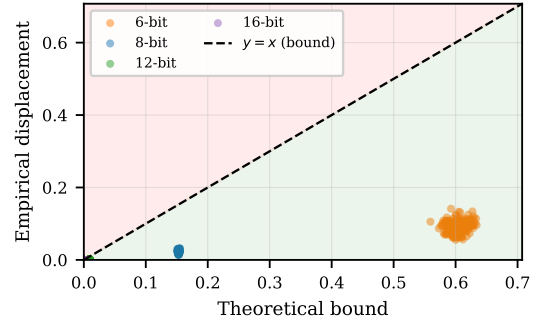


Fig. 2. Displacement bound validation (Theorem 3) at 6, 8, 12, and 16 bits. Each point is one test sample (x -axis: theoretical bound $(\|\Delta W\|_2/m) \|\tilde{z}^*\|_2$; y -axis: empirical displacement $\|\tilde{z}^* - z^*\|_2$). Points below the dashed line ($y = x$) satisfy the bound.

QAT vs. PTQ. Theorem 5 guarantees that the backward solve converges whenever the forward solve does; this makes QAT well-defined, since it requires differentiating through the equilibrium. Figure 3 compares PTQ and QAT at 4, 6, and 8 bits. At 4 bits, PTQ fails ($\tilde{m} = -0.142$). QAT succeeds by learning weights that satisfy $\tilde{m} = 0.006 > 0$ (Figure 3, right), achieving 96.78% accuracy, though at the cost of a smaller margin ($m = 0.184$ vs. 0.227). At 6 and 8 bits, both methods converge, with PTQ achieving slightly higher accuracy (98.25% and 98.29%) because it inherits the larger float margin.

Displacement bound validation. The preceding experiments test *convergence*; we now test the *accuracy* of the converged equilibrium. Theorem 3 bounds the displacement $\|\tilde{z}^* - z^*\|_2 \leq (\|\Delta W\|_2/m) \|\tilde{z}^*\|_2$. Since the forward-

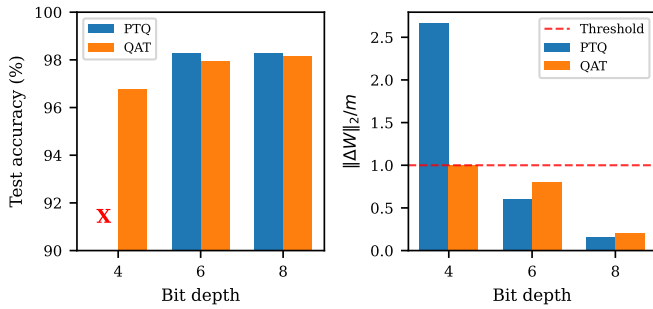


Fig. 3. QAT vs. PTQ at 4, 6, and 8 bits. Left: test accuracy (%; a red X indicates PTQ non-convergence at 4 bits). Right: $\|\Delta W\|_2/m$; the dashed line marks $\|\Delta W\|_2/m = 1$.

backward solver terminates at finite tolerance, the computed equilibrium approximates but does not equal the true \tilde{z}^* ; the theorem applies to the latter. Figure 2 evaluates the bound on 2,560 randomly sampled test inputs at 6, 8, 12, and 16 bits. The bound is satisfied in 99.1% (6-bit) to 91.3% (16-bit) of samples, with the empirical displacement 3–5 \times below the bound on average. The violation rate increases at higher bit-widths because $\|\Delta W\|_2$ shrinks and the bound tightens, while the absolute solver error from finite tolerance remains roughly constant. Corollary 3 gives a relative bound: at 16 bits, $\|\Delta W\|_2/(m - \|\Delta W\|_2) = 0.057\%$; at 6 bits, this rises to 154%, which is vacuous — the relative bound becomes non-trivial around 8 bits.

VI. CONCLUSIONS

We have analyzed the effect of weight quantization on monotone operator equilibrium networks through spectral perturbation of the monotone inclusion. The monotonicity margin m emerges as the single quantity governing robustness to quantization: convergence of the forward and backward solvers is guaranteed provided $\|\Delta W\|_2 < m$ (Theorem 2), the equilibrium displacement satisfies $\|\tilde{z}^* - z^*\|_2 \leq (\|\Delta W\|_2/m) \|\tilde{z}^*\|_2$ (Theorem 3), and the relative condition number $\kappa_{\text{rel}} = \|W\|_2/m$ links bit-width to forward error (Theorem 4). Experiments confirm a phase transition at the predicted threshold and show the displacement bound holds in 91–99% of test samples with a conservative factor of 3–5 \times . Quantization-aware training recovers convergence at 4 bits where post-training quantization fails, enabled by the backward-pass guarantee of Theorem 5.

The present analysis is limited to uniform symmetric quantization of a single-layer MonDEQ. Natural extensions include per-channel and mixed-precision schemes, multi-layer architectures, and margin-aware regularization during quantization-aware training to enforce a target bit-width a priori. An important open question is whether the behavioral guarantees of MonDEQ-based controllers [7], [8] remain valid under weight quantization; the present perturbation bounds are a first step toward such results.

ACKNOWLEDGMENT

Generative AI was used to assist with the experimentation code, finding references, and checking for grammatical

errors.

REFERENCES

- [1] M. Nagel, M. Fournarakis, R. A. Amjad, Y. Bondarenko, M. van Baalen, and T. Blankevoort, “A white paper on neural network quantization,” 2021, arXiv:2106.08295.
- [2] Y. Zhang, F. Song, and J. Sun, “QEBVerif: Quantization Error Bound Verification of Neural Networks,” in *Computer Aided Verification*, C. Enea and A. Lal, Eds. Cham: Springer Nature Switzerland, 2023, pp. 413–437.
- [3] A. Kabaha and D. D. Cohen, “Quantization with Guaranteed Floating-Point Neural Network Classifications,” *Proc. ACM Program. Lang.*, vol. 9, no. OOPSLA2, pp. 340:1893–340:1920, Oct. 2025.
- [4] M. Fu and L. Xie, “The sector bound approach to quantized feedback control,” *IEEE Transactions on Automatic Control*, vol. 50, no. 11, pp. 1698–1711, 2005.
- [5] E. Winston and J. Z. Kolter, “Monotone operator equilibrium networks,” in *Advances in Neural Information Processing Systems*, vol. 33, 2020.
- [6] S. Bai, J. Z. Kolter, and V. Koltun, “Deep equilibrium models,” in *Advances in Neural Information Processing Systems*, vol. 32, 2019.
- [7] M. Revay, R. Wang, and I. R. Manchester, “Lipschitz bounded equilibrium networks,” 2020, arXiv:2010.01732.
- [8] —, “Recurrent Equilibrium Networks: Flexible Dynamic Models With Guaranteed Stability and Robustness,” *IEEE Transactions on Automatic Control*, vol. 69, no. 5, pp. 2855–2870, May 2024.
- [9] T. Chaffey, “Circuit realization and hardware linearization of monotone operator equilibrium networks,” Sep. 2025, arXiv:2509.13793.
- [10] N. J. Higham, *Accuracy and Stability of Numerical Algorithms*, 2nd ed. SIAM, 2002.
- [11] B. Jacob, S. Kligys, B. Chen, M. Zhu, M. Tang, A. Howard, H. Adam, and D. Kalenichenko, “Quantization and training of neural networks for efficient integer-arithmetic-only inference,” in *2018 IEEE/CVF Conference on Computer Vision and Pattern Recognition (CVPR)*, 2018, pp. 2704–2713.
- [12] J. Eckstein and D. P. Bertsekas, “On the Douglas—Rachford splitting method and the proximal point algorithm for maximal monotone operators,” *Mathematical Programming*, vol. 55, no. 1, pp. 293–318, Apr. 1992.
- [13] P. L. Combettes and J.-C. Pesquet, “Proximal Splitting Methods in Signal Processing,” in *Fixed-Point Algorithms for Inverse Problems in Science and Engineering*, H. H. Bauschke, R. S. Burachik, P. L. Combettes, V. Elser, D. R. Luke, and H. Wolkowicz, Eds. New York, NY: Springer, 2011, pp. 185–212.
- [14] T. Beuzeville, A. Buttari, S. Gratton, and T. Mary, “Deterministic and probabilistic rounding error analysis of neural networks in floating-point arithmetic,” *IMA Journal of Numerical Analysis*, 2025.
- [15] J. A. Jonkman, T. Sherson, and R. Heusdens, “Quantisation Effects in Distributed Optimisation,” in *2018 IEEE International Conference on Acoustics, Speech and Signal Processing (ICASSP)*, Apr. 2018, pp. 3649–3653.
- [16] C. Pabbaraju, E. Winston, and J. Z. Kolter, “Estimating Lipschitz constants of monotone deep equilibrium models,” in *International Conference on Learning Representations*, 2021.
- [17] E. K. Ryu and S. Boyd, “A primer on monotone operator methods,” *Applied and Computational Mathematics*, vol. 15, no. 1, pp. 3–43, 2016.
- [18] H. H. Bauschke and P. L. Combettes, *Convex Analysis and Monotone Operator Theory in Hilbert Spaces*, ser. CMS Books in Mathematics. Cham: Springer International Publishing, 2017.
- [19] A. L. Dontchev, A. Eberhard, and R. T. Rockafellar, “Radius Theorems for Monotone Mappings,” *Set-Valued and Variational Analysis*, vol. 27, no. 3, pp. 605–621, Sep. 2019.
- [20] R. A. Horn and C. R. Johnson, *Matrix Analysis*. Cambridge: Cambridge University Press, 1985.
- [21] T. Beuzeville, “Backward error analysis of artificial neural networks with applications to floating-point computations and adversarial attacks,” Ph.D. dissertation, Université de Toulouse, 2024.
- [22] P. L. Combettes and J.-C. Pesquet, “Deep neural network structures solving variational inequalities,” *Set-Valued and Variational Analysis*, vol. 28, pp. 491–518, 2020.